SPECT of Serotonin Transporters Using ^{123}I-ADAM: Optimal Imaging Time After Bolus Injection and Long-Term Test–Retest in Healthy Volunteers

Ana M. Catafau, MD, PhD[1,2]; Víctor Pérez, MD, PhD[3]; María M. Penengo, MSc[1]; Santiago Bullich, PhD[1]; Mónica Danús, MD[1]; Dolors Puigdemont, MD[3]; Juan C. Pascual, MD[3]; Iluminada Corripio, MD[3]; Jordi Llop, PhD[4]; Javier Perich, MD, PhD[5]; and Enric Álvarez, MD, PhD[3]

[1]Centre for Imaging in Psychiatry, CRC–Mar, Hospital del Mar, Barcelona, Spain; [2]Experimental Medical Sciences, Clinical Pharmacology Discovery Medicine, Psychiatry Centre of Excellence for Drug Discovery, GlaxoSmithKline, Barcelona, Spain; [3]Psychiatry Department, Hospital Sant Pau, Barcelona, Spain; [4]Radiochemistry Laboratory, Institut d'Alta Tecnologia, Barcelona, Spain; and [5]Magnetic Resonance Department, CRC–Mar, Hospital del Mar, Barcelona, Spain

^{123}I-ADAM (2-([2-([dimethylamino]methyl)phenyl]thio)-5-^{123}I-iodophenylamine) has been recently proposed as a new serotonin transporter (SERT) ligand for SPECT. The objective of this study was to characterize ^{123}I-ADAM in healthy volunteers. ^{123}I-ADAM distribution in the normal brain, pseudoequilibrium interval after a single injection, normal specific uptake values, and long-term test–retest variability and reliability were investigated. **Methods:** Ten healthy volunteers underwent 2 SPECT sessions under the same conditions 47.6 ± 24.0 d apart. Scans were sequentially acquired from the time of ^{123}I-ADAM intravenous injection up to 12 h after injection. Regions of interest (ROIs) for cerebellum (C), midbrain, thalamus, striatum, mesial temporal region, and cortex were drawn on MR images and pasted to corresponding SPECT slices after coregistration. Specific uptake ratios (SURs) at pseudoequilibrium and the simplified reference tissue model (SRTM) methods were used for quantification. SURs were obtained as ([region $-$ C]/C) at each time point. Test–retest variability and reliability (intraclass correlation coefficient [ICC]) were calculated. **Results:** The highest ^{123}I-ADAM specific uptake was found in the midbrain and thalamus, followed by the striatum and mesial temporal region. Quantification results using SUR and SRTM were correlated with $R = 0.93$ (test) and $R = 0.94$ (retest). SURs remained stable in all regions from 4 to 6 h after injection. Using SUR, test–retest variability/ICC were $13\% \pm 11\%/0.74$ in midbrain, $16\% \pm 13\%/0.63$ in thalamus, $19\% \pm 18\%/0.62$ in striatum, and $22\% \pm 19\%/0.05$ in mesial temporal region. **Conclusion:** ^{123}I-ADAM accumulates in cerebral regions with high known SERT density. The optimal imaging time for ^{123}I-ADAM SPECT quantification is suggested to be from 4 to 6 h after a single injection. Long-term test–retest variability and reliability found in the midbrain are comparable to that reported with other ^{123}I-labeled SPECT ligands. These results support the use of ^{123}I-ADAM SPECT for SERT imaging after a single injection in humans.

Key Words: ^{123}I-ADAM; SPECT; test–retest; serotonin transporter

Imaging of serotonin transporters (SERTs) in the living human brain by means of SPECT has been limited because of the lack of a selective SERT radioligand. ^{123}I-β-CIT (2β-carbomethoxy-3β-(4-^{123}I-iodophenyl)tropane), previously used for SERT measurements, binds to both dopamine and serotonin transporters, thus lacking selectivity (1). Recently, ^{123}I-ADAM (2-([2-([dimethylamino]methyl)phenyl]thio)-5-^{123}I-iodophenylamine) has been identified as a SPECT ligand with high SERT affinity (rat cortical membrane homogenates, dissociation constant [K_d] = 0.15 ± 0.03 nmol/L [mean $\pm$ SD]) (2) and >1,000-fold selectivity for SERT over norepinephrine transporter and dopamine transporter (2,3). Biodistribution and radiation dosimetry data of ^{123}I-ADAM in healthy volunteers support its use in humans (4,5).

Given the widespread availability of SPECT, SERT imaging using ^{123}I-ADAM could become a promising tool for human studies. SERT density has been reported as a surrogate marker for serotonergic neuronal loss, as occurring in neurodegenerative diseases (6) and ecstasy users (7–9). Moreover, SERT plays a role in mood disorders, and pharmacologic actions of the selective serotonin reuptake inhibitors (SSRIs) used as antidepressants are based on SERT blockade. Performance of 2 SPECT scans on the same subject weeks to months apart (i.e., at diagnosis and at follow-up or baseline and after treatment) are required for a proper assessment of SERT availability changes over time. Knowledge of test–retest variability is crucial for interpre-

tation of the results. Given that neurodegeneration is a slow process and that 4–6 wk are typically required for SSRIs to show clinical efficacy, long-term test–retest variability and reliability are of particular interest.

Quantification of SERT availability using the simple ratio method has been correlated with full kinetic modeling in a baboon study (10). A single SPECT scan acquisition at pseudoequilibrium after a single bolus injection and quantification using the simple ratio method are the approaches of choice in a clinical setting, to maximize patient compliance and performance feasibility in most SPECT centers. The aims of the present study were, first, to characterize ^{123}I-ADAM as a SPECT SERT ligand in healthy volunteers (i.e., to investigate its distribution in the normal brain, the pseudoequilibrium interval, and normal specific uptake values in different cerebral regions) and, second, to assess long-term test–retest variability and reliability. The radioligand behavior in plasma was additionally studied in 5 subjects.

MATERIALS AND METHODS

Subjects

Ten healthy volunteers (7 males, 3 females; mean age ± SD, 36.2 ± 10.6 y; range, 28–65 y) participated in this study. Inclusion criteria included no clinical history of neurologic or psychiatric diseases or drug abuse and normal physical examination and review of systems. Pregnancy was excluded in females by means of a urine pregnancy test (Clearview HCG II; Unipath Limited).

The study was approved by the local Ethics Committees and the Ministry of Health. In all cases, written informed consent was obtained before inclusion in the study.

Study Design and SPECT Protocol

Each subject underwent 2 SPECT scans under the same conditions 47.6 ± 24.0 d apart. Four multimodality SPECT/MRI markers (MM3003; IZI Medical Products Corp.), each filled with approximately 0.074 MBq (2 μCi) of ^{123}I, were attached to the subject's head at the level of the temples and mastoids to allow for SPECT and MRI coregistration and realignment of SPECT images from different times. Potassium perchlorate (8 mg/kg) was administered orally up to 20 min before radioligand injection to minimize radiation exposure to the thyroid gland. ^{123}I-ADAM (170.7 ± 25.3 MBq; MAP-Findland, OY) was injected intravenously and flushed with 20 mL of saline solution. In 5 subjects, a venous catheter was inserted in a forearm vein on the opposite arm for blood sampling. Dynamic ^{123}I-ADAM acquisitions were performed with a triple-head Prism 3000S camera (Philips) fitted with ultrahigh-resolution fanbeam collimators. The scans were collected using a 360° circular orbit, step-and-shoot mode every 3°, on a matrix size of 128 × 128 pixels. For both test and retest sessions, acquisitions started at 0–1, 2, 3, 4, 5, 6, and 7 h after injection in all subjects. An additional scan at 9 h after injection was obtained in 8 subjects and at 12 h after injection in 5 subjects. Four 15-min scans were acquired for the first hour after injection, and subsequent 30-min scans were acquired every other hour with 30-min breaks in between.

MRI

Each subject underwent MRI on the day of each SPECT scan for coregistration and region-of-interest (ROI) drawing and place-

ment. A superconductive 1.9-T system (Prestige 2T; GE Healthcare) with a head coil was used. An axial 3-dimensional spoiled gradient-echo slab was positioned to include the entire head, and images were acquired with the following parameters: repetition time, 25 ms; echo time, 6 ms; flip angle, 28°; field of view, 25 × 25 cm; matrix size, 256 × 256; section thickness, 2 mm with no interslice gap; and number of excitations, 1. Pixel size was 0.97 mm in the transaxial direction and 2 mm in the axial direction.

Image Analysis

Images were reconstructed using a filtered-backprojection algorithm with a Butterworth filter (exponent = 5.0; cuttoff frequency = 0.4 cycle/pixel). Pixel sizes were between 2.5 and 2.8 mm on each slice and 3.6 mm in the axial direction. Chang's algorithm was applied for attenuation correction (coefficient = 0.1 cm^{-1}). SPECT and MRI scans were coregistered using in-house software implemented in C language and were resliced before the registration to obtain a homogeneous pixel size of 0.97 mm in each direction. The centroid positions of the fiducial markers were used to coregister SPECT to MRI using a 6-parameter (3 translation and 3 rotation) rigid-body transformation by minimizing the least squares of the distance of the corresponding marker positions (11).

ROIs were manually drawn on the MR image on cerebellum, midbrain, thalamus, striatum, and mesial temporal region, frontal, temporal, parietal, and occipital cortex. Sampled volumes for the ROIs used are presented in Table 1.

Two methods were used for quantification: the simple ratio method and the simplified reference tissue model (SRTM) (12). For the simple ratio method, the specific uptake ratio (SUR) was calculated as measurement of the specific-to-nonspecific partition coefficient at each time point: ([R − C]/C), where R is the mean counts in a cerebral region and C is the mean counts in the region of reference (cerebellum). SURs were also calculated using only 1 set of ROIs drawn on the first-day MR image. For this purpose, the SPECT–MRI coregistration of the second day was subsequently coregistered with the first-day MRI using the mutual information–based algorithm as implemented in the SPM2 software package (Wellcome Department of Cognitive Neurology, Institute of Neurology, University College London) (11,13). For SRTM, binding potential (BP) was calculated from the time–activity curves between 0 and 360 min after injection by using in-house software implemented in C language: BP[unitless] = $f_2 \cdot B_{max}/K_d$, where f_2 is the free fraction of the nonspecific distribution volume in the brain and B_{max} is the maximum number of binding sites.

Plasma Analysis

Plasma analysis of ^{123}I-ADAM was performed in 5 subjects. A total of 17 venous blood samples were collected manually at times −1, 0.25, 0.5, 1, 1.5, 2, 5, 10, 15, 30, 45, 120, 180, 240, 300, 360, and 420 min after injection. The first blood sample was extracted as a reference. Samples 2–17 were separated in 2 fractions (1 mL each), introduced into 1.5-mL flasks, and centrifuged at 2,000g for 4 min. The plasma fraction was separated and both plasma and residue fractions were counted in a γ-counter (2200 Scaler Ratemeter; Ludlum Measurements Inc.). All samples were further processed by analytic high-performance liquid chromatography (HPLC) to determine the fraction of plasma activity representing unmetabolized radiotracer. For this purpose, 1 mL of pure acetonitrile was added to the plasma fraction and, after mixing, the samples were centrifuged at 2,000g for 4 min. The liquid phase was separated from the precipitate by decantation, and both fractions were counted in the γ-counter to determine the activity

TABLE 1
Sample Volumes of ROIs Used for Analysis at Test and Retest

ROI volume	Test Mean ± SD (cm³)	100 · SD/mean	Retest Mean ± SD (cm³)	100 · SD/mean	% dif
Cerebellum	79.4 ± 8.9	11.2	80.5 ± 5.5	6.9	1.3
Midbrain	5.3 ± 1.1	21.4	5.8 ± 0.8	14.2	9.1
Thalamus	13.4 ± 3.4	25.2	13.2 ± 3.6	27.2	−1.4
Striatum	13.8 ± 2.5	18.1	13.8 ± 1.8	12.9	0.0
Mesial temporal	29.2 ± 5.8	19.8	29.8 ± 5.3	17.8	2.1
Frontal	84.1 ± 30.6	36.4	71.6 ± 16.4	22.9	−16.1
Temporal	93.5 ± 27.3	29.2	80.7 ± 16.9	21.0	−14.7
Parietal	49.4 ± 12.1	24.5	50.6 ± 16.3	32.1	2.4
Occipital	47.2 ± 14.3	30.3	36.3 ± 8.9	24.6	−26.2

% dif = percentage of difference in mean ROI volumes between test and retest.

fraction linked to protein. For HPLC analysis, both protein-free fractions corresponding to the same blood sample were joined, and the resulting solution was evaporated at 40°C under continuous helium flow. The residue was diluted in 100 μL of mobile phase acetonitrile/water, 60:40, and injected into the HPLC system, consisting of an Agilent 1100 series chromatograph, and equipped with a 1100 series isocratic pump, a Rheodyne injector with a 20-μL loop, a temperature-controlled column compartment (temperature set point = 25°C), a ZORBAX Eclipse XDB-C8 column (4.6 × 150 mm, 15 μm), and a γ-detection system (GABI; Raytest) equipped with a 100-μL flow cell. The whole system was controlled by Gina-Star Raytest software. The detection energy window was adjusted to 159 ± 50 keV. The chromatographic runs were performed under isocratic conditions (acetonitrile/water, 60:40), at a flow of 1 mL/min, with a total chromatographic time of 10 min. Between 2 consecutive injections, mobile phase was circulated at 1 mL/min for 10 min.

From the first blood sample, two 1-mL samples were separated and introduced in 1.5-mL flasks, and 100 μL of ^{123}I-ADAM reference solution (activity concentration ∼ 1.85 MBq/mL, measured with a Capintec dose calibrator, COMECER) were added to each flask. The resulting solutions were submitted to the same experimental procedure as described for samples 2–17. Sample 1 was used to determine retention time of the parent compound under chromatographic conditions and to calculate the relation between activity concentration in plasma and counts obtained in the γ-counter. All samples were processed within 60 min after blood sampling.

Statistical Analysis

Summaries of study variables were expressed as mean ± SD. SPSS/PC for Windows (version 11 0.1, 2001) was used for statistical analysis. Test–retest variability was calculated as the mean of the absolute differences of test minus retest divided by the mean of test and retest expressed in percent. The reliability of the 2 sets of measurements was assessed by the intraclass correlation coefficient (ICC): ICC = ([MSBS − MSWS]/[MSBS + (k − 1)MSWS]), where MSBS and MSWS are the mean sum of squares between and within subjects, respectively, and k is the number of repeated observations ($k = 2$ in this study).

A 2-way repeated-measures ANOVA was performed with condition (test, retest) and scan time as factors to test for the main effects of these 2 variables on the SUR for each region. A post hoc analysis (Dunn test) was used to identify the starting and ending time points of the pseudoequilibrium interval (i.e., the time interval in which SURs are not significantly different).

A paired t test was used for comparison of the test–retest variability obtained using 1 and 2 sets of ROIs. In all cases, a 2-tailed $P = 0.05$ was selected as the significance level.

RESULTS

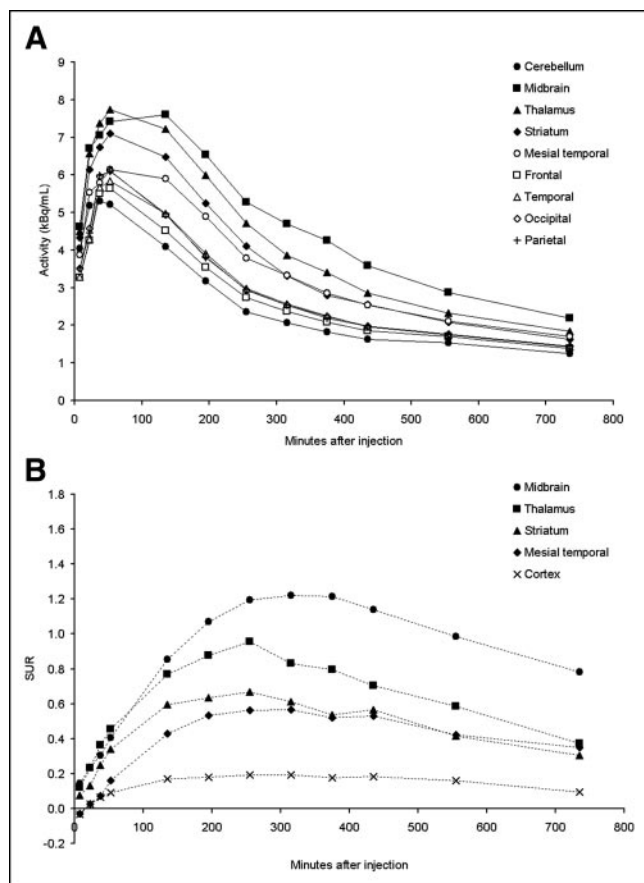### ^{123}I-ADAM Brain Distribution, Pseudoequilibrium Interval, and SURs

SPECT images in Figure 1 show the distribution of ^{123}I-ADAM in the normal brain. The highest uptake was found in the midbrain, followed by the thalamus. Striatum and mesial temporal regions showed a moderate ADAM uptake, and cortical regions showed very faint uptake.

Mean time–activity curves from the 20 SPECT examinations performed on the 10 healthy volunteers showed that the activity in cerebellum peaked between 15 and 30 min after injection; cortical regions peaked between 30 and 45
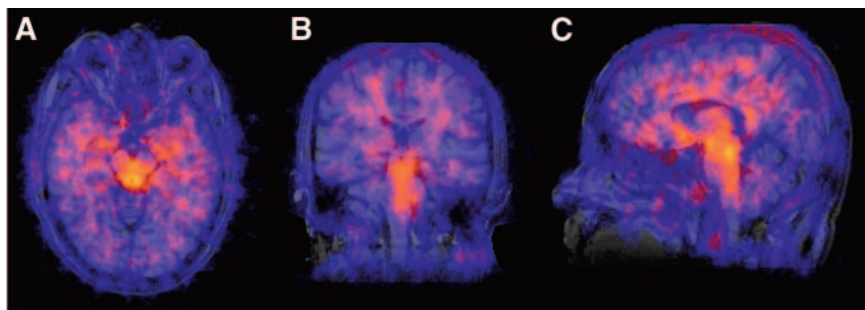
FIGURE 1. Coregistered MRI–SPECT images show ^{123}I-ADAM distribution in representative healthy volunteer (added images from 4 to 6 h after injection). (A) Axial slice shows high specific ^{123}I-ADAM uptake in midbrain and moderate uptake in mesial temporal region. Coronal (B) and sagittal (C) slices show high uptake in midbrain and thalamus and moderate uptake in striatum. Note predominant uptake in dorsal part of midbrain on sagittal view.

min after injection, showing slightly higher values than the cerebellum. Finally, the regions showing high and moderate ^{123}I-ADAM uptake—that is, midbrain, thalamus, striatum, and mesial temporal region—peaked between 45 and 60 min after injection (Fig. 2A). The 2-way repeated-measures ANOVA revealed no significant effect of condition on any region ($P > 0.2$ for all regions), but the overall effect of time was significant for all tested regions (midbrain: $F_{23} = 23.07$, $P < 0.01$; thalamus: $F_{23} = 9.06$, $P < 0.01$; striatum: $F_{23} = 7.38$, $P < 0.01$; mesial temporal region: $F_{23} = 14.79$, $P < 0.01$). Mean SUR–time curves from the 20 SPECT examinations performed are shown in Figure 2B. Stable SURs (i.e., not showing statistically significant differences) were obtained between 4 and 7 h after injection for the midbrain, between 3 and 6 h after injection for the thalamus, and between 3 and 7 h after injection for the striatum and mesial temporal region. Therefore, mean SURs for each region were calculated for the 4- to 6-h postinjection interval, which was identified as the common pseudoequilibrium interval for all regions. Normal SURs and BPs calculated

TABLE 2
Mean SURs at Pseudoequilibrium and BP Using SRTM for Regions Showing High and Moderate ^{123}I-ADAM Uptake

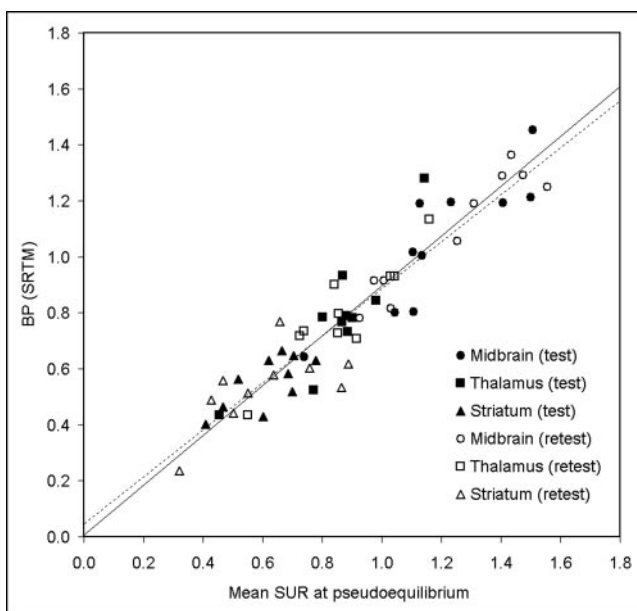| Region	SUR	BP (SRTM)
Midbrain	1.21 ± 0.24	1.07 ± 0.22
Thalamus	0.86 ± 0.20	0.79 ± 0.20
Striatum	0.61 ± 0.18	0.54 ± 0.11
Mesial temporal	0.55 ± 0.12	0.42 ± 0.11

All values are mean ± SD of all 20 scans ($n = 10$ subjects, test and retest scans).
SUR = specific uptake ratio; BP (SRTM) = binding potential (simplified reference tissue model).

using SRTM are shown in Table 2. Cortical regions showed very faint uptake, with SURs ≤ 0.21. A linear correlation was found between quantification results obtained using the simple ratio and the SRTM methods (Fig. 3), although mean SURs were consistently higher than BPs obtained with SRTM.

^{123}I-ADAM SPECT Test–Retest Variability and Reliability

SUR–time curves obtained at test and retest are shown in Figure 4. Test–retest variability and reliability (ICC) results are presented in Table 3. No statistically significant differences were found between the test–retest variability of SUR calculated using 1 and 2 sets of ROIs. However, a slight improvement was consistently found in ICC values when only 1 set of ROIs was used. The midbrain was the region

FIGURE 2. (A) Mean time–activity curves for each cerebral region obtained from 20 SPECT examinations performed on 10 healthy volunteers. (B) Mean time–SUR curves for each cerebral region obtained from 20 SPECT examinations performed on 10 healthy volunteers. Cortex curve is mean of all cortical regions. In A and B, 540- and 720-min scans were based on 8 and 5 subjects, respectively.

FIGURE 3. Scatter plot of parameters obtained using ratio method (mean SUR from 4 to 6 h after injection) and SRTM. Continuous line corresponds to linear fitting for test data (BP test = 0.89 SURtest + 0.01, $R = 0.93$). Dashed line corresponds to linear fitting for retest data (BP retest = 0.84 SURretest + 0.05, $R = 0.94$).
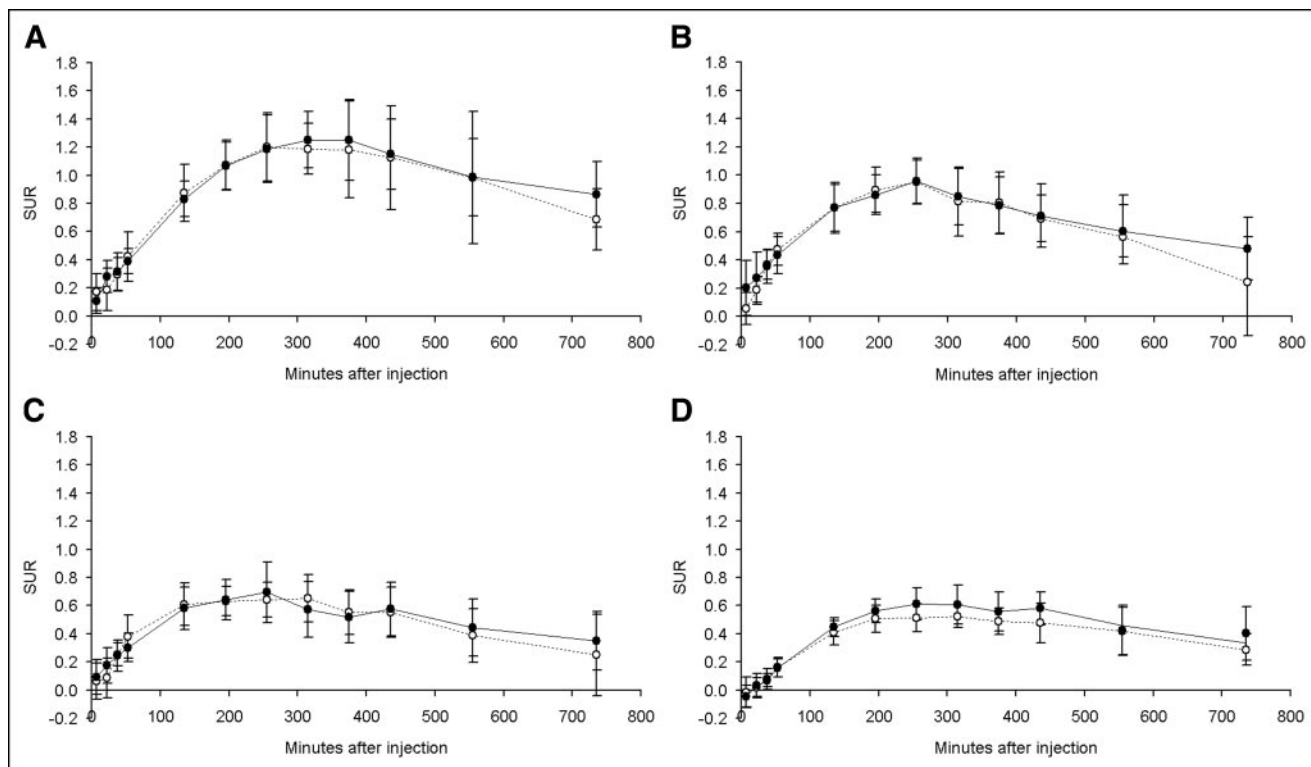
FIGURE 4. Mean time–SUR curves at test (○) and retest (●) for regions showing high (midbrain [A] and thalamus [B]) and moderate (striatum [C] and mesial temporal region [D]) ¹²³I-ADAM specific binding. The 540- and 720-min scans were based on 8 and 5 subjects, respectively.

showing the lowest test–retest variability and the highest ICC. Thalamus and striatum showed similar ICC values, although test–retest variability was lower in the thalamus. The mesial temporal region, which showed the lowest specific uptake values, was the region showing the poorer test–retest variability and ICC (Fig. 4; Table 3).

Plasma Analysis

Total plasma activity and the fraction of activity corresponding to the unmetabolized parent compound in the plasma as a function of time are presented in Figure 5. Both activity values reach a plateau after a rapid distribution phase. The percentage of unmetabolized parent compound as a function of time is

presented in Figure 6A. At the end of the study (time = 420 min) only $5.46\% \pm 1.8\%$ of the activity present in the plasma free fraction is due to the parent compound. Moreover, after 10 min, the fraction of the activity corresponding to the unmetabolized parent compound in plasma represents only <20% of total plasma free fraction activity. Figure 6B shows the chromatograms obtained for samples 1, 6, and 16 (−1, 2, and 360 min after injection). Besides the parent compound, only 2 species could be detected in the first chromatogram (reference); both species are more hydrophilic than the parent compound. Comparison of the chromatograms shows that the relative size of the peak with a retention time ≈ 2 min increases

TABLE 3
Mean Test–Retest Variability and ICC Corresponding to SUR Calculated Using 1 and 2 Different Sets of ROIs (Means from 4 to 6 Hours After Injection) and BP (SRTM) for Regions Showing High and Moderate ¹²³I-ADAM Uptake ($n = 10$)

	Test–retest variability (%)				ICC		
Region	SUR (2 ROI sets)	SUR (1 ROI set)	P*	BP (SRTM)	SUR (2 ROI sets)	SUR (1 ROI set)	BP (SRTM)
Midbrain	13.16 ± 11.17	13.55 ± 12.13	0.73	13.99 ± 7.20	0.70 ± 0.03	0.74 ± 0.02	0.74
Thalamus	16.39 ± 13.55	14.78 ± 13.95	0.22	12.75 ± 12.15	0.63 ± 0.06	0.66 ± 0.10	0.78
Striatum	19.23 ± 17.91	17.92 ± 15.23	0.40	15.56 ± 15.32	0.62 ± 0.14	0.64 ± 0.14	0.66
Mesial temporal	21.68 ± 19.21	24.26 ± 18.45	0.09	31.01 ± 33.42	0.05 ± 0.10	0.17 ± 0.04	0.12

*Paired t test P value (comparison between SUR (2 ROI sets) and SUR (1 ROI set)).
ICC = intraclass correlation coefficient; SUR = specific uptake ratio; BP (SRTM) = binding potential (simplified reference tissue model).
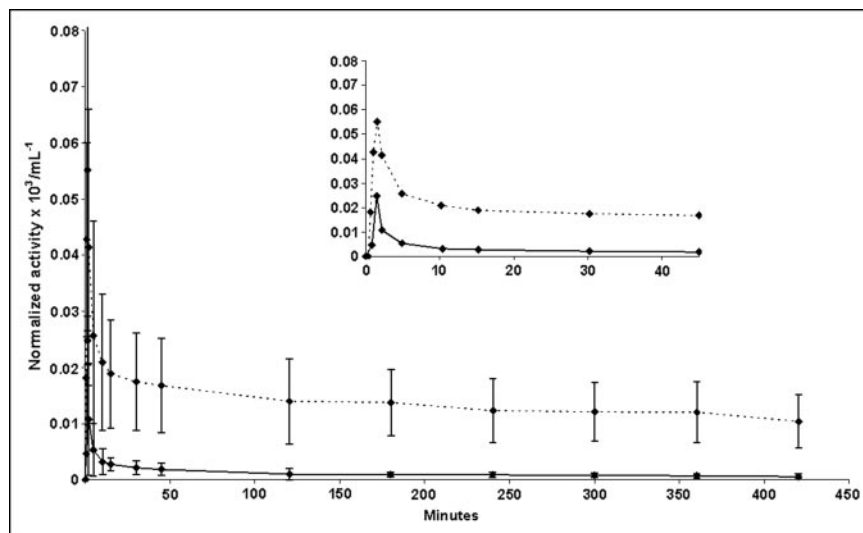
FIGURE 5. Total plasma activity (dotted line) and activity corresponding to unmetabolized parent compound (straight line) in plasma as function of time, decay-corrected to injection time. Values shown are averages calculated from data obtained in 5 healthy volunteers.

with time, whereas the peak with a retention time ≈ 2.8 min disappears in samples taken at time ≥ 2 min. The peak at time ≈ 5.5 min (corresponding to unmetabolized parent compound) decreases in size over time until it reaches a relative size of $5.46\% \pm 1.8\%$ of total activity in the free fraction at time $= 420$ min. Although there is no experimental evidence of the structure of the radioactive metabolites, coinjection with unlabeled iodine showed the same retention time with the first peak (retention time ≈ 2). The free fraction of the activity present in plasma versus time (referred to total plasma activity) is shown in Figure 7. After an initial decrease, a plateau at around 75% is reached.

DISCUSSION

^{123}I-ADAM Brain Distribution, Pseudoequilibrium Interval, and SURs

Distribution of ^{123}I-ADAM found in this study is in close agreement with the anatomic localization of SERT binding sites described with autoradiography in the human brain (14), showing high densities of SERT in the raphe nuclei of the midbrain and upper pons and in the thalamus, followed by the basal ganglia, hippocampus, and amygdala. Low SERT density in the neocortex and very low density in the cerebellum were also reported (14). ^{123}I-ADAM time–activity curves showed early peak uptake in the low SERT density regions and later peak uptake in high SERT density regions (Fig. 2A). Literature reporting ^{123}I-ADAM uptake in the normal human brain is still limited, most of it having been published as abstracts (5,15–17). Reported results are summarized in Table 4. The time selected for quantification analysis after a single bolus injection varies among authors from 150 to 300 min after injection. The present study has shown variability in the pseudoequilibrium intervals among cerebral regions. SURs stabilized from 180 min in the thalamus, striatum, and mesial temporal regions and from 240 min after injection in the midbrain (Fig. 2B). In all
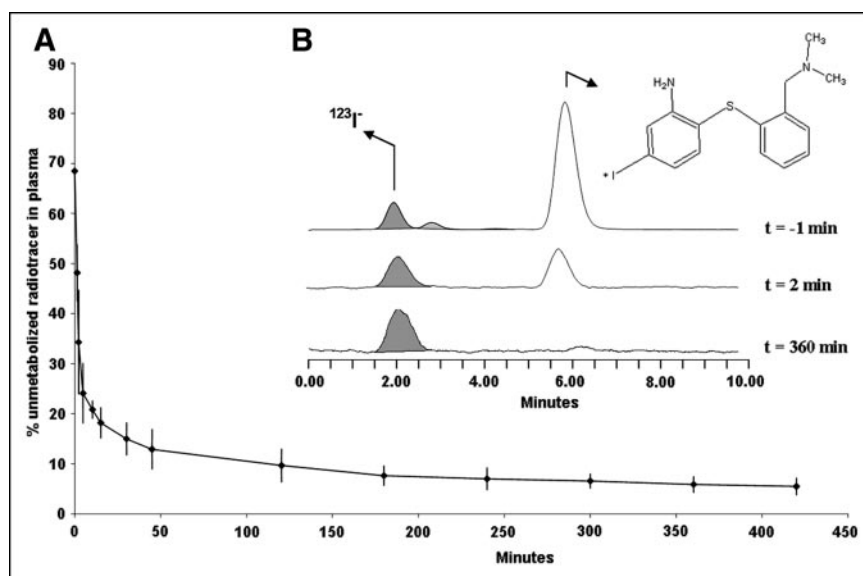
FIGURE 6. (A) Percentage of unmetabolized parent compound in plasma as function of time. (B) Chromatograms obtained for samples extracted at time $= -1$ min, 2 min, and 360 min after injection.
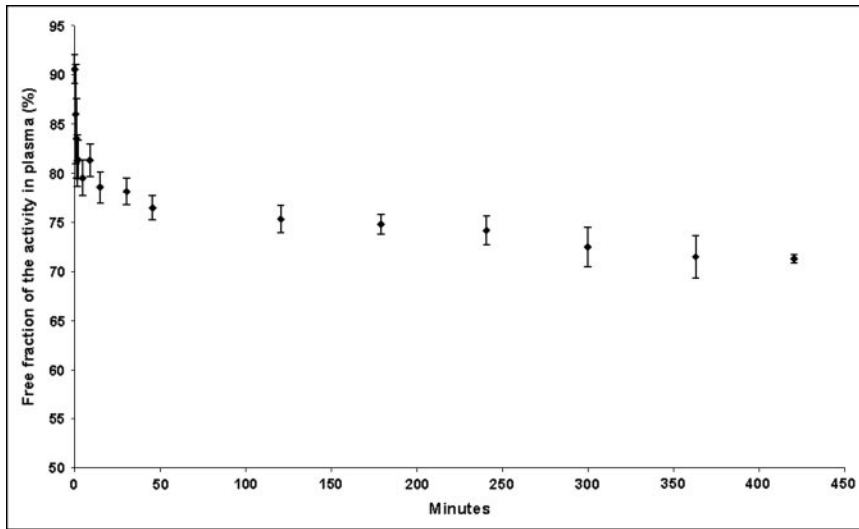
FIGURE 7. Free fraction of activity present in plasma (percentage referred to total plasma activity) vs. time.

cases, SUR remained stable at least up to 360 min after injection. It is known that the time required to reach equilibrium is dependent on the density of receptors (*18*). The raphe nuclei, which are included in the midbrain ROI, contain the highest SERT density in the brain. Therefore, longer time is required to reach equilibrium in this region. The present study shows a common pseudoequilibrium interval for all regions from 4 to 6 h after injection, suggesting that this is the optimal time for scan acquisition and SUR quantification after single bolus injection. From 7 to 12 h after injection, SURs decreased progressively, but a higher variability in the measurements was also observed. Sample size differences in later time points (9 and 12 h after injection) could have influenced the ANOVA results and, hence, the definition of the pseudoequilibrium interval. However, this seems unlikely since no statistically significant differences were found when comparing the mean SURs obtained at 7 h after injection between the group of

subjects who completed the 12-h scanning ($n = 5$) and those who did not ($n = 5$) (Mann–Whitney U test, $P > 0.3$ for all regions). The higher variability found in the 9- and 12-h postinjection measurements could partially be explained by the lower sample sizes and by the faint activity in these scan acquisitions given the radioisotope decay. Therefore, it is not possible to completely rule out a possibility of a longer pseudoequilibrium interval.

Independently from the scan acquisition time selected for quantification, all authors have consistently reported the midbrain as the area showing the highest specific ^{123}I-ADAM uptake, with SURs ranging from 0.95 to 1.7 (Table 4). Comparison of SURs across studies in Table 4 is potentially limited by methodologic differences between them, including scanner resolution and sensitivity, reconstruction parameters, attenuation and scatter corrections, SPECT–MRI coregistration, and the ROI method used. Heterogeneity in the distribution of SERT in a particular cerebral region

TABLE 4
Summary of SURs Reported in Literature Using ^{123}I-ADAM SPECT in Healthy Volunteers

Reference	n	Age (y)	Scan acquisition interval (min after injection)	^{123}I-ADAM uptake value Midbrain	Thalamus	Striatum	Mesial temporal	Cortex
9	7	22–54	210–270	1.95 ± 0.3 (0.95*)	NA	1.11 ± 0.07 (0.11*)	1.27 ± 0.1 (0.27*)	NA
18	6	30–42	150–210	2.1–2.7 (1.1–1.7*)	2.2 (1.2*)	2.0 (1.0*)	NA	1.3 (0.3*)
17	9	23–55	300	1.61 ± 0.35	NA	NA	NA	NA
19	12	22–62	210†	1.21 ± 0.12	NA	NA	NA	NA
This study	10‡	28–65	240–360	1.21 ± 0.24	0.86 ± 0.20	0.61 ± 0.18	0.55 ± 0.12	≤0.21

*Values in parentheses are calculated as ([target/cerebellum ratio] − 1) for those articles originally reporting target/cerebellum ratios, to allow comparison with SURs (target − cerebellum/cerebellum).

†No decline of SUR up to last scan acquired at 300 min after injection.

‡SUR calculated from 20 SPECT examinations performed on 10 subjects.

NA = not available.

may also contribute. For example, human brain autoradiography has revealed the highest SERT density in the nucleus raphe dorsalis (*14*). Therefore, smaller ROIs drawn on the posterior part of the midbrain may give higher SURs than larger ROIs including the whole structure. The midbrain ROI is the smallest of the ROIs drawn in this study, as shown in Table 1. Moreover, it is the most difficult ROI to delineate on MRI, given that the contour of the midbrain is not easy to identify. These factors may account for the 9% difference between the midbrain ROI volume drawn at test and at retest, which was far the highest difference found among the ROI volumes in the regions with specific ^{123}I-ADAM uptake (Table 1). Therefore, the use of the MRI–SPECT coregistration method—drawing the ROIs on the MR images instead of drawing ROIs directly on SPECT images—is advisable to obtain more comparable and reproducible results, particularly in the midbrain.

The cerebellum (reference region) ROI was the largest of the ROIs used for SUR calculation and the ROI showing a lower coefficient of variance (Table 1). The larger the ROI volumes in the reference region, the lower the noise and the lower the variability in the SURs. The cerebellum has been consistently chosen as a reference region for SUR calculation. Although low SERT density is present in this region (*14*), it has been reported that ^{123}I-ADAM activity in the cerebellum is not displaced by citalopram, therefore supporting its use as the reference region (*19*).

Finally, 2 quantification methods were compared in this study. A good correlation between SUR and SRTM was found, although higher values were consistently found for SUR (Table 2). This is in full agreement with the preliminary results from Erlandsson et al. (*20*). In baboons, it has been shown that SRTM underestimates the BP and has a bias such that the underestimation increases with higher binding (*10*). Without a metabolite-corrected arterial input function, both SRTM and SUR provide an estimation of regional SERT specific binding. Nevertheless, the use for the quantification of SERT without arterial blood sampling has been supported by a correlation found between full kinetic modeling and SRTM in a preliminary study in humans (*19*).

^{123}I-ADAM SPECT Test–Retest Variability and Reliability

To the best of our knowledge, this is the first time that ^{123}I-ADAM SPECT test–retest variability and reliability are reported in humans. Test–retest variabilities reported in humans with other ^{123}I-labeled neurotransmission SPECT ligands are in line with those found for the midbrain using ^{123}I-ADAM in the present study. A 10%–17% variability has been reported for SPECT measurement of benzodiazepine receptors using ^{123}I-iomazenil, depending on the outcome measure and the fitting procedure (*21*). Using ^{123}I-epidepride for extrastriatal D2 receptors, variability/reliability have been reported as 13.3%/0.75 for the thalamus and 13.4%/0.86 for the temporal cortex (*22*). Test–retest variabilities of 11.1% ± 10.4% for subdivided striatal ROIs and 11.9% ± 1.22% for whole striatal ROIs has been reported using ^{123}I-FPCIT (^{123}I-Ioflupane) for D2 receptor quantification, with reliabilities of 0.59 and 0.65, respectively (*23*). The test–retest variability of ^{123}I-β-CIT has been reported to be 12% ± 9% for the dopamine transporter measurements, although, again, differences were found depending on the fitting strategy of the quantification model (*24*). No published data on the variability of ^{123}I-β-CIT for the SERT measurement in humans have been found for comparison.

In this study, similar test–retest variability results were obtained using either 1 or 2 sets of ROIs on the same subject. However, a slightly higher reliability (ICC) should be expected if the same set of ROIs is used for within-subject comparisons. Although SUR and SRTM quantification methods correlated well, a slightly better reliability was found with the SRTM. However, a total of 7 scans from 0 to 360 min after injection were needed for the quantification, which most likely would be unfeasible to apply in patients in most SPECT centers. Therefore, quantification using SUR is proposed as more suitable for human studies.

Plasma Analysis

^{123}I-ADAM stability in plasma has been recently reported by Stahr et al. (*25*) in 6 healthy volunteers, suggesting that <1% of the parent compound is likely to be metabolized within the 60 min after blood sampling. Our samples were processed within the 60 min after extraction; thus, the maximum error due to this processing delay should be <1%.

Plasma analysis of ^{123}I-ADAM has been previously reported in both nonhuman primates (*10*) and humans (*25*). Acton et al. (*10*) found that, after 6 h, the unmetabolized parent compound in plasma represented only 5.7% of the total plasma activity in baboons (*n* = 3). However, arterial blood samples were analyzed and, therefore, only results at long times after injection are comparable with those obtained in the present work. Stahr et al. (*25*) found that fractional unchanged ^{123}I-ADAM varied from subject to subject, being around 5%–12% at 3–4 h after injection. Moreover, unidentified lipophilic metabolites were detected in some subjects.

As shown in our work, and in agreement with the results obtained by Stahr et al. (*25*), ^{123}I-ADAM is highly metabolized in human subjects (only 5.46% ± 1.8% of the total plasma free fraction activity was found to correspond to unmetabolized parent compound at the end of the study; Fig. 6A), suggesting that decomposition of the parent compound should be considered when calculating the input function. Besides the parent compound, only 1 species could be detected in the chromatograms at time > 2 min, corresponding to a more hydrophilic species than the parent compound (probably iodine) and, thus, not supposed to cross the blood–brain barrier. No hydrophobic metabolites were found in any of subjects' samples.

The initial decrease of the free fraction of the activity present in plasma, as shown in Figure 7, can be explained by (i) iodine has a higher affinity for protein than ADAM. The increase in the percentage of iodine due to metabolization of the parent compound leads to this decrease in the free plasma fraction; or (ii) the linking process to protein is slow and the relative decrease observed for the unmetabolized parent compound in the free fraction is due, partly, to the linking process of ADAM to protein.

CONCLUSION

^{123}I-ADAM accumulates in cerebral regions with high known SERT density, showing a high specific uptake in the midbrain and thalamus and moderate uptake in the striatum and mesial temporal region. The optimal time interval for SPECT after a single bolus injection is from 4 to 6 h after injection. The correlation found between the SUR and SRTM quantification methods supports the use of SUR as the simplest method, avoiding the need for blood sampling and serial scanning over time. ^{123}I-ADAM SPECT quantification using SUR will make the technique suitable in more centers and will allow larger groups of patients to be scanned. Plasma analysis showed a high and fast metabolization of ^{123}I-ADAM. No lipophilic metabolites were found for any of the subjects. The poor variability and reliability found in the mesial temporal region suggests that it is not a suitable region for SERT assessment using ^{123}I-ADAM SPECT. On the other hand, the long-term test–retest variability and reliability of ^{123}I-ADAM SPECT in the midbrain are comparable with other ^{123}I-labeled SPECT ligands. This supports the midbrain as a suitable region to monitor long-term SERT availability changes using ^{123}I-ADAM SPECT in humans.

REFERENCES

1. Laruelle M, Baldwin RM, Malison RT, et al. SPECT imaging of dopamine and serotonin transporters with [123]beta-CIT: pharmacological characterization of brain uptake in nonhuman primates. *Synapse.* 1993;13:295–309.
2. Oya S, Choi SR, Hou C, et al. 2-((2-((Dimethylamino)methyl)phenyl)thio)-5-iodophenylamine (ADAM): an improved serotonin transporter ligand. *Nucl Med Biol.* 2000;27:249–254.
3. Choi SR, Hou C, Oya S, et al. Selective in vitro and in vivo binding of [125]ADAM to serotonin transporters in rat brain. *Synapse.* 2000;38:403–412.
4. Kauppinen TA, Bergstrom KA, Heikman P, Hiltunen J, Ahonen AK. Biodistribution and radiation dosimetry of [123]ADAM in healthy human subjects: preliminary results. *Eur J Nucl Med Mol Imaging.* 2003;30:132–136.
5. Newberg AB, Plossl K, Mozley PD, et al. Biodistribution and imaging with ^{123}I-ADAM: a serotonin transporter imaging agent. *J Nucl Med.* 2004;45:834–841.
6. Berding G, Brucke T, Odin P, et al. [^{123}I]Beta-CIT SPECT imaging of dopamine and serotonin transporters in Parkinson's disease and multiple system atrophy. *Nuklearmedizin.* 2003;42:31–38.
7. Reneman L, Booij J, Habraken JB, et al. Validity of [123]beta-CIT SPECT in detecting MDMA-induced serotonergic neurotoxicity. *Synapse.* 2002;46:199–205.
8. Thomasius R, Petersen K, Buchert R, et al. Mood, cognition and serotonin transporter availability in current and former ecstasy (MDMA) users. *Psychopharmacology (Berl).* 2003;167:85–96.
9. de Win MM, Reneman L, Reitsma JB, den Heeten GJ, Booij J, van den Brink W. Mood disorders and serotonin transporter density in ecstasy users: the influence of long-term abstention, dose, and gender. *Psychopharmacology (Berl).* 2004;173:376–382.
10. Acton PD, Choi SR, Hou C, Plossl K, Kung HF. Quantification of serotonin transporters in nonhuman primates using [123]ADAM and SPECT. *J Nucl Med.* 2001;42:1556–1562.
11. Bullich S, Ros D, Pavia J, et al. Influence of co-registration algorithms on ^{123}I-IBZM SPET imaging quantification [abstract]. *Eur J Nucl Med Mol Imaging.* 2004;31(suppl):S49.
12. Lammertsma AA, Hume SP. Simplified reference tissue model for PET receptor studies. *Neuroimage.* 1996;4:153–158.
13. Maes F, Collignon A, Vandermulen D, Suetens P. Multimodality image registration by maximization of mutual information. *IEEE Trans Med Imaging.* 1997;16:187–198.
14. Cortes R, Soriano E, Pazos A, Probst A, Palacios JM. Autoradiography of antidepressant binding sites in the human brain: localization using [3H]imipramine and [3H]paroxetine. *Neuroscience.* 1988;27:473–496.
15. Ahonen AK, Kauppinen TA, Heikman P, et al. Imaging of serotonin transporters in human beings using ^{123}I-ADAM [abstract]. *J Nucl Med.* 2002;43(suppl):232P.
16. Asenbaum S, Fuger B, Diemling M, Dudczak R. ^{123}I-ADAM SPECT: a new method for investigating serotonin transporter in humans [abstract]. *Eur J Nucl Med Mol Imaging.* 2003;30(suppl):S309.
17. Dresel S, la Fougere C, Makowski M, et al. Imaging of the serotonin transporter in healthy controls: pharmacodynamics of ^{123}I-ADAM [abstract]. *J Nucl Med.* 2004;45(suppl):261P.
18. Olsson H, Halldin C, Swann CG, Farde L. Quantification of [11C]FLB 457 binding to extrastriatal dopamine receptors in the human brain. *J Cereb Blood Flow Metab.* 1999;19:1164–1173.
19. Frokjaer VG, Pinborg LH, Madsen J, Knudsen GM. Evaluation of the serotonin transporter ligand ^{123}I-ADAM for SPECT studies in humans [abstract]. *Neuroimage.* 2004;22(suppl):T176.
20. Erlandsson K, Sivananthan T, Lui D, et al. Estimation of SSRI occupancy of sert using the novel SPET tracer ^{123}I-ADAM and simultaneous modeling [abstract]. *Neuroimage.* 2004;22(suppl):T144.
21. Abi-Dargham A, Gandelman M, Zoghbi SS, et al. Reproducibility of SPECT measurement of benzodiazepine receptors in human brain with iodine-123-iomazenil. *J Nucl Med.* 1995;36:167–175.
22. Varrone A, Fujita M, Verhoeff NP, et al. Test-retest reproducibility of extrastriatal dopamine D2 receptor imaging with [123]epidepride SPECT in humans. *J Nucl Med.* 2000;41:1343–1351.
23. Tsuchida T, Ballinger JR, Vines D, et al. Reproducibility of dopamine transporter density measured with ^{123}I-FPCIT SPECT in normal control and Parkinson's disease patients. *Ann Nucl Med.* 2004;18:609–616.
24. Seibyl JP, Laruelle M, van Dyck CH, et al. Reproducibility of iodine-123-beta-CIT SPECT brain measurement of dopamine transporters. *J Nucl Med.* 1996;37:222–228.
25. Stahr K, Frokjaer VG, Knudsen GM. Evaluation of a metabolite assay: quantification of [I123] ADAM in human plasma [abstract]. *Eur J Nucl Med Mol Imaging.* 2004;31(suppl):S485.